Tribology Letters, Vol. 25, No. 3, March 2007 (© 2006)
DOI: 10.1007/s11249-006-9166-9

XPS study of the influence of temperature on ZnDTP tribofilm composition

Roman Heuberger[a], Antonella Rossi[a,b] and Nicholas D. Spencer[a,*]

[a]*Laboratory for Surface Science and Technology, Department of Materials, ETH Zurich, Wolfgang-Pauli-Strasse 10, Zurich, CH-8093, Switzerland*

[b]*Dipartimento di Chimica Inorganica ed Analitica, Università degli Studi di Cagliari, INSTM Research Unit, Cittadella Universitaria di Monserrato, Cagliari, I-09100, Italy*

Received 4 August 2006; accepted 17 October 2006; published online 30 November 2006

Antiwear additives, such as zinc dialkyldithiophosphate (ZnDTP), find application in many different industrial sectors. Although it is understood that certain ZnDTP concentrations need to be used to achieve an effective antiwear performance, there has been very little work published concerning the effect of temperature on the interactions of the additive and its adsorption mechanism on steel. In this article, 100Cr6 (52100) steel ball-on-disc experiments under solutions of zinc dialkyldithiophosphate (ZnDTP) in poly-α-olefin (PAO) were performed at different temperatures, ranging from 25 to 180 °C. The discs were analysed after the experiments by means of small-area, imaging and angle-resolved X-ray photoelectron spectroscopy (XPS). The composition of the reaction film was found to change as a function of the applied temperature and also to vary within the film as a function of depth: Longer polyphosphate chains were found at higher temperatures as well as towards the outer part of the reaction film.

KEY WORDS: XPS, ZnDTP, boundary lubrication, tribochemistry

1. Introduction

The oil temperature in automobile engines varies considerably during a typical journey. It begins at ambient temperature when starting the engine and increases to 80–100 °C under normal use. At higher engine loads, the temperature can locally increase up to 150 °C or even higher [1,2]. In addition, very high contact pressures are present in an engine, which render lubrication challenging, e.g. 1–2 GPa in the case of cam and follower [1,3,4]. The most widely used extreme-pressure additives—used to protect such components against wear—are zinc dialkyldithiophosphates (ZnDTP) [5]. Initially introduced in the 1940s as antioxidants, they impart excellent antiwear properties by forming a protective film on the rubbing surfaces. These films have been extensively investigated by means of X-ray photoelectron spectroscopy (XPS) [6–8], X-ray absorption spectroscopy [8–10] and *in situ* attenuated total reflection infrared spectroscopy [11,12], among many other methods. Although much effort was put into understanding the antiwear mechanism, there are still open questions concerning film formation, the reacting species, the reaction kinetics and the presence of a viscous layer on the film and its composition [5].

Temperature has a significant influence on the course of the reaction. The thermal degradation of ZnDTPs occurs between 130 and 230 °C. It has been suggested that it begins with a migration of the alkyl groups (which were bound on the oxygen atom of the thiophosphate) to the sulphur atoms [13,14], and indications of these intermediate molecules were also suggested by Fuller *et al.* for thermal films produced at 100 °C [15]. Following attack by a neighbouring phosphoryl group, a poly(thio)phosphate is formed, accompanied by the release of an alkyl sulphide species [5,16]. Under tribological conditions, reaction films are formed even at room temperature [7,17,18] but the composition is reported to change with increasing temperature from zinc phosphate to zinc polyphosphate [6,8,11,12]. Changes in elemental concentrations and chain length of the phosphate chains with depth have been observed by means of XANES (sampling depth from 5 nm up to >5 μm, depending on the applied mode) [8,19,20] as well as by depth profiling with argon-sputtering [8].

In a polyphosphate (see scheme in figure 1) there are two types of oxygen atoms that can be distinguished by XPS: the bridging oxygen (BO) linking two phosphate groups together (P–O–P) and the non-bridging oxygen (NBO) terminating the phosphates ($-PO_x$) [21]. Thus, the ratio of BO to NBO allows the chain length n of the (poly)phosphate to be calculated, and therefore provides important information on the structure of the formed film.

So far, film formation has normally been investigated at 25, 80 and 150 °C and there is a lack of information

*To whom correspondence should be addressed.
E-mail: spencer@mat.ethz.ch

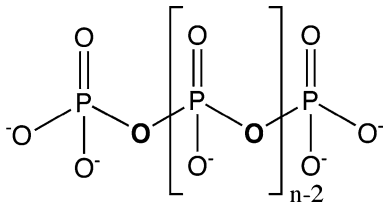

Figure 1. Scheme of a polyphosphate with the chain length *n*. The oxygen atoms linking two phosphorus atoms together (bold) are called bridging oxygen (BO), while the terminal oxygen atoms in the phosphate groups are called non-bridging oxygen (NBO) [21].

concerning the changes in chemical states of the elements and in their relative ratios as a function of depth. In this work, the influence of temperature on the composition of both tribological and thermal films has been investigated by mean of small-area and angle-resolved XPS (ARXPS), in order to yield three-dimensional information. Special attention has been paid to the chemical structure of the (poly)phosphate and its chain length.

2. Experimental

2.1. Tribological testing

For the ball-on-disc test a CETR UMT-2 tribometer with temperature control up to 180 °C was used (Center for Tribology, Campbell, CA, USA). Both ball and disc (both hardened bearing steel 100Cr6, 52100) were fully immersed in the lubricant oil. A 1 wt.% solution of a commercial secondary zinc dialkyldithiophosphate ZnDTP (C_3H_7 + C_6H_{13}, see figure 2, HiTEC®7169, Afton Chemical Corporation, Richmond VA, USA, purified by liquid chromatography) in poly-α-olefin (PAO, Durasyn 166, Tunap Industries GmbH. & Co., Mississauga, Canada) was used as a lubricant. Tests were performed at 25, 60, 90, 100, 110, 130, 150 and 180 °C (all ±3 °C). The relative humidity was between 23 and 44%. Prior to the actual test, a running in of the ball on a designated region of the disc with a load of 5 N was performed for 2 h. In order to produce a tribo-stressed area of adequate size for subsequent XPS analysis with the PHI 5700 or Theta Probe instruments, a step test with 11 or 3 steps was run, as described in ref. [22]. In total, 11 steps were chosen for the samples measured with the PHI 5700 (Aperture: 120 μm; see Section 2.3) and three steps were used prior to analysis with the Theta Probe (spot size: 30 μm). Each step consists of five turns with 5 N load and 31.4 mm/min sliding speed; the step size was 25 μm. Before further investigation, the sample was rinsed and ultrasonically cleaned with ethanol (p.a.) for 3 min.

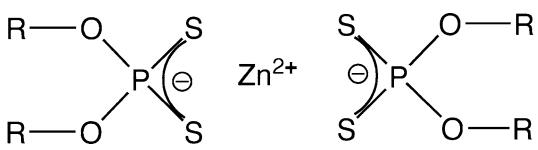

Figure 2. Chemical formula of zinc dialkyldithiophosphate (ZnDTP).

2.2. Optical microscopy

Optical microscopy images were taken using a Reichert-Jung Polyvar microscope (Leica Microsystems Nussloch GmbH, Wetzlar, Germany) with objectives from 5× to 100× and equipped with a CCD camera (Leica Microsystems GmbH, Wetzlar, Germany).

2.3. X-Ray photoelectron spectroscopy

X-Ray photoelectron spectroscopy measurements on small areas (contact regions and non-contact areas) were conducted in a PHI 5700 (Physical Electronics, Chanhassen MN, USA), while ARXPS spectra were measured with a Theta Probe (Thermo Electron Corporation, Waltham MA, USA).

The PHI 5700 is equipped with an Omni Focus lens system. The source was AlKα (1486.6 eV), run at 350 W. The diameter of the analysed area was 120 μm. The analyser was operated in the fixed-analyser-transmission mode with a pass energy of 46.95 eV (full width at half-maximum (fwhm) for $Ag3d_{5/2}$ = 1.1 eV). Spectroscopic images were measured by electronically rastering the analysed spot over the sample. The images were displayed and processed with PHI Multipak V6.0 software and the points of interest chosen according to the resulting intensity distribution.

The Theta Probe is equipped with a radian lens and a two-dimensional detector that collects the electrons, which are discriminated for signal intensities in both photoelectron energy and photoemission angle. Eight simultaneous emission angles were acquired ranging from 23° to 83° and 16 emission angles were used for acquiring the angle-resolved maps. Monochromatic, microfocused AlKα radiation with a spot size of 30 μm and a power of 6 W was used; the pass energy of the analyser was 200 eV. A nominal spectrometer energy resolution of 1.4 eV was used. By moving the translation stage, O1s spectra were recorded on 17 × 17 points over 500 × 500 μm. Combined with the 16 angle-dependent spectra/point, this resulted in a total of 4624 spectra. These were fitted with VG Avantage 3.19 software by constraining the binding energy of the oxide peak to be between 530.2 and 530.3 eV. The NBO was fixed to be 1.6 eV above the oxide peak, and the BO 3.1 eV above the oxide. The percentages of the individual oxygen peaks with respect to the sum of all oxygen peaks were plotted in 2D-maps, which were then used to create the 3D-plots (Adobe Illustrator CS2).

The residual pressure in both spectrometers during the measurement was always below 5×10^{-7} Pa. The systems were calibrated according ISO 15472:2001 and the accuracy was better than ± 0.05 eV.

High-resolution spectra taken on the chosen points were processed with Casa XPS Software (V2.3.5, Casa Software Ltd., UK). In the case of $Fe2p_{3/2}$ measured with non-monochromatic AlKα, the satellite originating from the $Fe2p_{1/2}$ peak was subtracted with the CasaXPS software. An iterated Shirley-Sherwood background subtraction was applied prior to the curve fitting. Curve-fitting parameters were determined from reference spectra acquired under the same analysis conditions [7] and the spectra fitted with a linear-least-squares algorithm. If the ratio of the fwhm of the peaks on the sample to the fwhm of the reference spectrum was found to be higher than 1.15 (a number derived from statistical fwhm analysis of over 50 spectra), then this was taken as an indication that an additional peak should be introduced in the curve synthesis. Sample charging had to be corrected for the samples tribostressed at 180 °C, referring all binding energies to aliphatic carbon at 284.8 eV. This value is the average binding energy measured for the C1s signals collected on thermal and tribostressed samples at lower temperature. The thickness and composition of the layers were calculated applying a three-layer model [23], where the peak areas were corrected for the photoionisation cross-section σ_i according to Scofield [24], the analyser transmission function $T(E_i)$ of the instrument [25], the density of the model compound ρ divided by the atomic weight of the element A_i, the inelastic mean free path (IMFP) $\lambda(E_i)$ according to Tanuma *et al.* [26,27] and $\cos(\theta)$, where θ is the emission angle (see figure 3). The three layers were iron oxide as a semi-infinite substrate, covered with the reaction layer, which, in turn, was coated with an organic layer. The model compounds for the calculations of the IMFP and the density in the layer model are given in table 1.

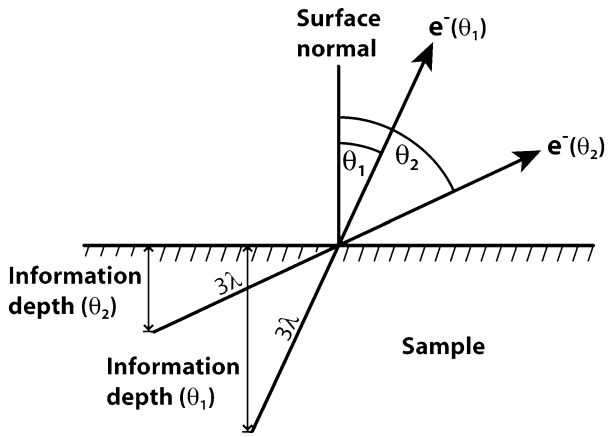

Figure 3. Scheme of the information depth in dependence of the emission angle θ for angle-resolved XPS measurements. The information depth is defined as the depth from where 95% of the detected electrons are coming from Ref. [49] and is equal to $3\lambda \cos(\theta)$, where λ is the inelastic mean free path [50]. Thus, the higher the emission angle, the smaller is the information depth and therefore the more surface sensitive is the measurement.

3. Results

3.1. Tribological tests

The colour plot of the friction coefficient μ for a step test (11 overlapping tracks with 5 turns) performed at 130 °C is shown in figure 4 (left). The friction force jumped to higher values every five turns due to the stepwise change of the tribotrack to a new one. It was necessary to perform a step test in order to produce a large tribostressed area for the following XPS analysis performed with an aperture diameter of 120 μm. The mean friction coefficient μ for different temperatures is shown in figure 4 (right). Starting from a low value of 0.14 ± 0.02 at room temperature, it increased with increasing temperatures to a high-friction regime for temperatures above 130 °C; here the friction coefficient was 0.20 ± 0.02, i.e. 45% higher than that at room temperature.

Optical microscopy of samples tribostressed in a step test clearly showed the 11 wear tracks close to each other (see figure 5). There was almost no visual difference between tribostressed samples from 25 to 150 °C—only tribostressed samples at 180 °C showed a brownish layer covering the non-contact area.

3.2. XPS results

Survey and high-resolution (detailed) spectra were recorded in the contact and the non-contact areas. In the survey spectra, only signals from phosphorus, sulphur, carbon, oxygen, iron and zinc were detected. Subsequently, detailed spectra of phosphorus P2p together with Zn3s, sulphur S2p, carbon C1s, oxygen O1s, iron Fe2p and zinc Zn2p were measured. As an example, the spectra from the contact region produced at 130 °C are shown in figure 6; corresponding spectra were also recorded for the non-contact areas.

The signals of phosphorus, sulphur, iron and zinc of the 2p orbital exhibit two peaks $2p_{3/2}$ and $2p_{1/2}$ due to spin-orbit splitting. The area of the $2p_{3/2}$ peak is always double that of the $2p_{1/2}$ peak and the binding energy of the $2p_{1/2}$ peak is the higher of the two peaks. In the *phosphorus* and *sulphur* signals these two peaks are close to each other, resulting in an asymmetric signal. The model curves used for fitting the experimental peaks were linked to each other: the ratio of $2p_{1/2}/2p_{3/2}$ contributions was fixed at 0.5 and the difference in energy was maintained equal to 1.25 eV for sulphur and 0.85 eV for phosphorus [7]. In addition to the phosphorus signal at 133.6 eV, a peak originating from zinc,

Table 1.
Model compounds used for calculating the inelastic mean free path (IMFP) and for the density in the three-layer model.

Layer	Model Compound	Formula	Temperature range	Density [g/cm3]	Band gap [eV]
Organic layer	Aliphatic carbon	$CH_3[CH_2]_nCH_3$	25–180 °C	1	5
Reaction layer	Zinc phosphate tetrahydrate	$Zn_3(PO_4)_2$*$4H_2O$	25–110 °C	3.04 [51]	3.4 [52]
	Zinc pyrophosphate	$Zn_2P_2O_7$	130–150 °C	3.75 [51]	3.4 [52]
	Zinc metaphosphate (amorph.)	$Zn(PO_3)_2$	180 °C	3.04 [53]	3.68 [52]
Oxide layer	Magnetite	Fe_3O_4	25–180 °C	5.17 [51]	3.0 [54]

Please note that for the reaction layer different compounds were used, depending on the experimental temperature.

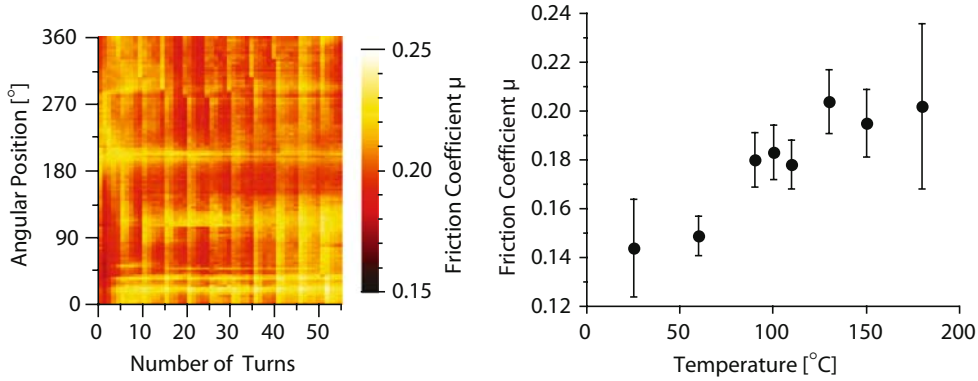

Figure 4. Colour plot of the friction coefficient μ as a function of the angular position on the sample and the number of turns (left). The sample was tribostressed in a step test at 130 °C. The increase of the friction coefficient every five turns was observed as the ball was moved to a new radius. Friction coefficient μ in dependence of the applied temperature (right).

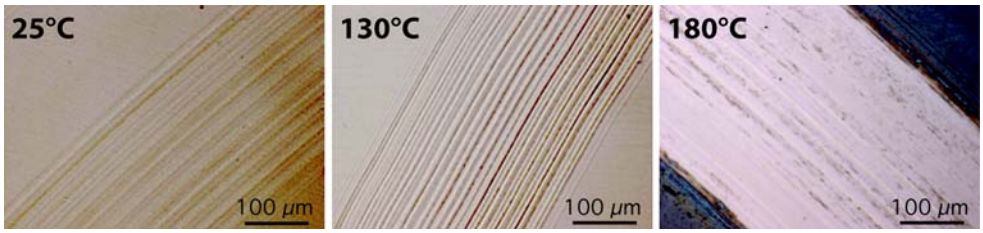

Figure 5. Optical microscopy images of samples tribostressed with a load of 5 N in a step test with 11 steps performed at 25, 130 and 180 °C.

Zn3s, was detected at 140 eV. In the case of sulphur, two different peaks, each composed of $S2p_{3/2}$ and $S2p_{1/2}$, were detected: one at 162.1 eV assigned to sulphides [7,28,29] and thiols [30,31] and one at 168.8 eV assigned to sulphate groups [29,32].

The most intense component in the *carbon* signal was from aliphatic carbon (C–C, C–H), found at 284.8 ± 0.1 eV. Minor contributions were found at 286.8 ± 0.2 and 289.1 ± 0.3 eV.

The *oxygen* signal consisted of three peaks at 530.2 ± 0.1 eV, 531.8 ± 0.1 eV and 533.4 ± 0.1 eV. The low-binding-energy peak at 530.2 eV is assigned to iron and zinc oxide [7,33,34]. The main peak at 531.8 eV originates from NBO in (poly)phosphates and from other groups such as sulphate, carbonate or hydroxides [7,35,36]. The peak at 533.4 eV is assigned to BO, which links phosphate groups together to form phosphate chains [35–37].

The *iron* spectra showed two main peaks with maxima of $Fe2p_{3/2}$ at 711 eV and of $Fe2p_{1/2}$ at 724 eV (spin-orbit splitting). Curve synthesis was performed only on the $Fe2p_{3/2}$ signal. The main components are the peaks from iron oxide, Fe(II) and Fe(III), at 709.6 and 710.9 eV, respectively, as well as the Fe(II)-satellite at 715.1 eV with 8% intensity of the main peak [7,34]. On the higher-binding-energy side there is another peak at 713.5 eV, which is assigned to iron phosphate [37].

The *zinc* spectra consist of the two peaks $Zn2p_{3/2}$ at 1022.4 eV and $Zn2p_{1/2}$ at 1045.8 eV (spin-orbit splitting).

3.3. Spectra at different temperatures

The shape of the spectra changed with temperature, and four regimes could be separated: 25 °C, 60–110 °C, 130–150 °C and 180 °C. Spectra of oxygen O1s in these

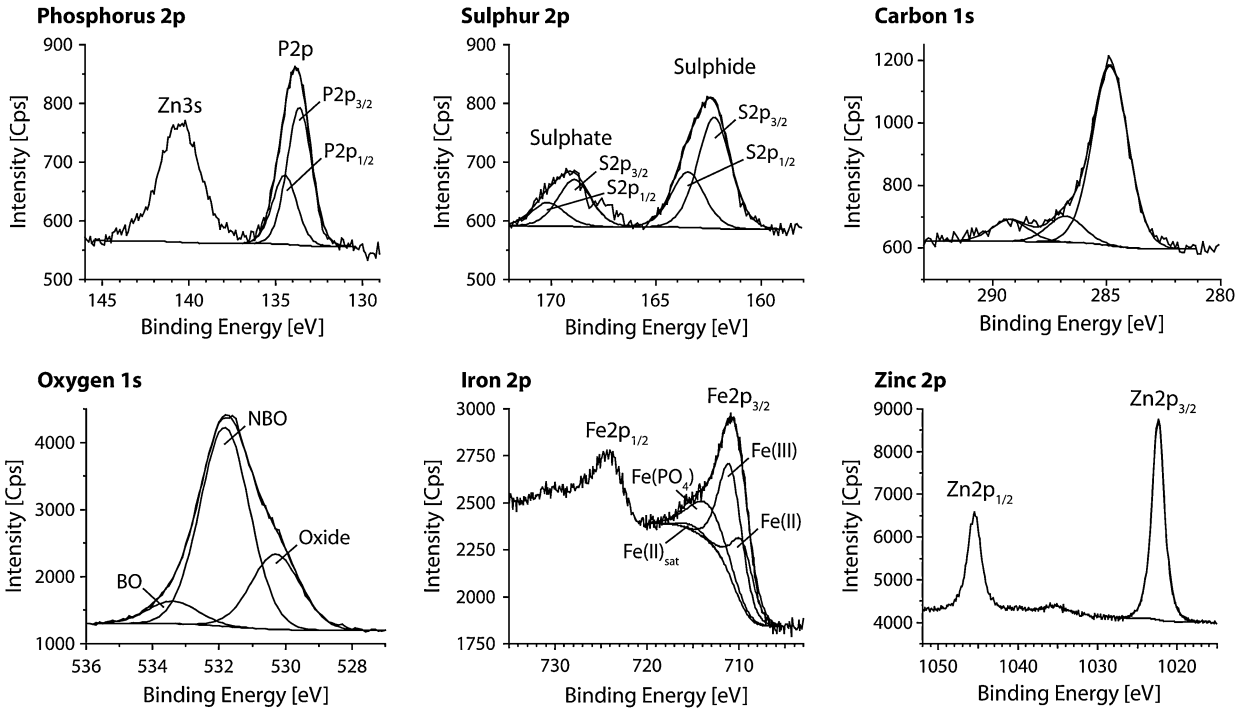

Figure 6. XPS detail spectra of P2p (with Zn3s), S2p, C1s, O1s, Fe2p and Zn2p of an area tribostressed with 5 N load at 130 °C (data acquired with PHI 5700). In the O1s contributions of NBO at 531.8 eV there are other contributions from sulphate, hydroxide or carbonate and in the BO there is, at low temperature, the contribution from water.

temperature regions are shown in figure 7 for the non-contact and for the tribostressed regions.

The main contribution to the oxygen signal measured on the *non-contact region* produced at *room temperature* came from iron oxide, together with a small contribution from zinc oxide. The iron spectra (not shown) exhibited peaks due to metallic iron (706.9 eV [7,33,34]), iron oxide and iron hydroxide (711.8 eV [7,34]). The signals of phosphorus, sulphur and zinc were detected only in trace amounts. As shown in figure 8, the binding

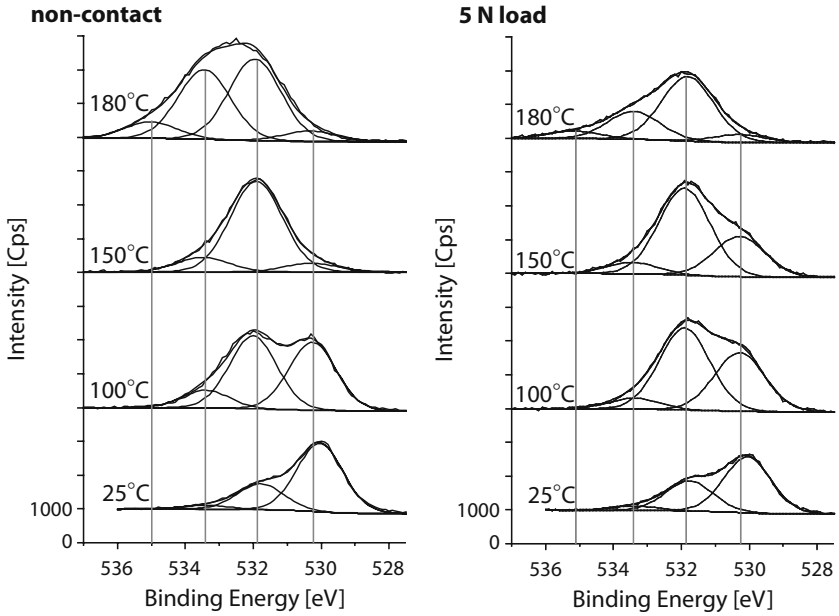

Figure 7. XPS detail spectra of oxygen 1s of non-contact films (left) and with 5 N tribostressed regions (right) formed at different temperatures. The signals consist of three peaks, one at 530.2 eV from the oxides, at 531.8 eV mainly from non-bridging oxygen and at 533.4 eV from bridging oxygen. At 180 °C an additional peak at 535 eV was observed likely due to oxygen linking phosphate chains together to form a cross-linked polyphosphate (data acquired with PHI 5700).

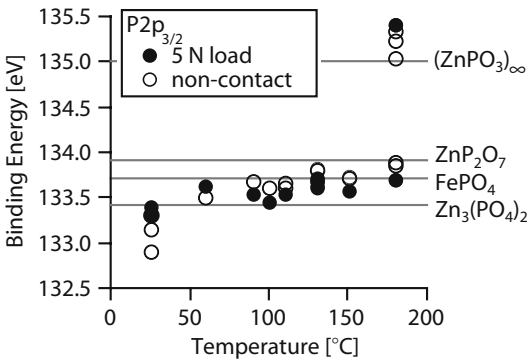

Figure 8. Binding energy of phosphorus $2p_{3/2}$ vs. temperature for areas tribostressed with 5 N load and the non-contact areas. Note that (only) at 180 °C there were two peaks at about 133.8 and 135.3 eV (fwhm of all peaks: 1.7 ± 0.1 eV) (data acquired with PHI 5700). Pinna [35] measured the reference compounds.

energy of phosphorus was lower compared to films produced at higher temperatures.

The spectra of the non-contact region in the *60–110* °C temperature range exhibited more prominent peaks of phosphorus, sulphur and zinc than at room temperature. In the oxygen spectra (figure 7 left, 100 °C) a higher contribution at 531.8 eV was detected, while the oxide peak was still significant.

Above *130* °C, the signals of the non-contact area showed more intense peaks of phosphorus, sulphur and zinc but less intense peaks of iron and O(oxide) compared to those of the contact regions (figure 6) and those taken at lower temperatures.

At *180* °C the signals for the non-contact region were broader and consisted of additional components: a peak at 535.0 ± 0.2 eV in the case of oxygen, one at 135.3 ± 0.2 eV in the case of phosphorus and one at 1023.7 ± 0.2 eV for zinc. The low-binding-energy peak of sulphur at 162.1 eV was shifted up to a higher binding energy of 163.6 ± 0.4 eV. The phosphorus signal was split into two doublets with binding energies of 133.9 ± 0.2 and at 135.2 ± 0.2 eV (see figure 8, fwhm 1.7 ± 0.1 eV). No iron was detected.

Different spectra of the elements described above were recorded in the *contact regions*. While the peak positions and shapes were similar to those from the non-contact region, major deviations in the peak areas were found: The tribostress at *room temperature* led to higher intensities of phosphorus, sulphur and zinc compared to the non-contact film. The spectra of the contact regions in the range of *60–110* °C had similar shapes as those at 130–150 °C (figure 6) but with smaller signals of the elements Zn, P and S, and more intense signals of Fe (also with metallic iron being detected) and of the O(oxide)-peak (figure 7). At 180 °C there were also small signals of iron oxide detected, which means that after the tribostress a thinner film was present than in the non-contact region.

3.4. 3D-colourplots of oxygen

Imaging-angle-resolved XPS was performed to obtain three-dimensional information about the tribofilm and the surrounding non-contact area. While imaging XPS provides lateral information, simultaneous angle-resolved measurements provide information on depth. A higher emission angle (angle between the analyser and the surface normal) corresponds to a higher surface sensitivity (see figure 3). The sample shown in figure 9 was tribostressed at 150 °C. At these temperatures, a thick tribofilm was formed, which provides a reasonable signal-to-noise-ratio of the oxygen peak for all 4624

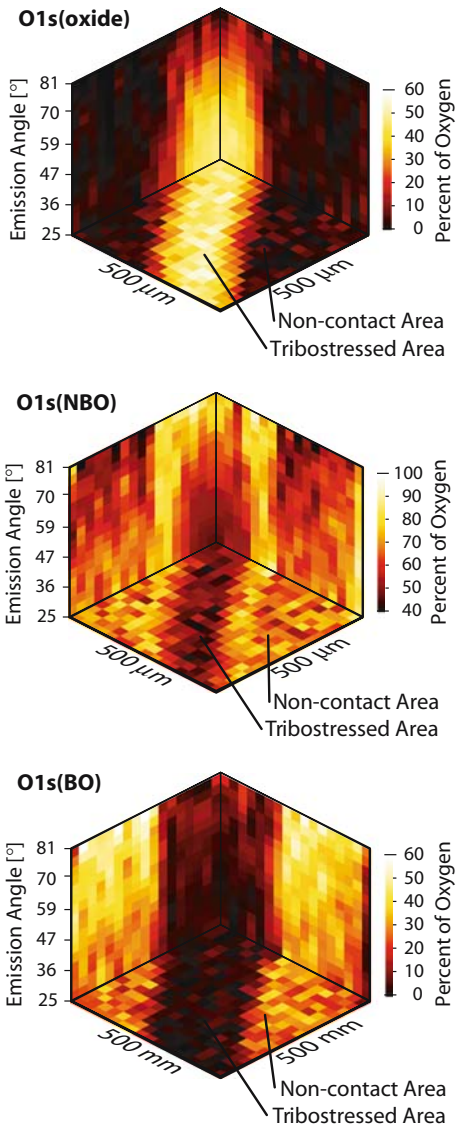

Figure 9. 3-D colour plots of the three oxygen peaks: oxide, non-bridging oxygen (NBO) and bridging oxygen (BO), measured on the tribostressed area and the surrounding non-contact area. The colour indicates the peak's percentage of the sum of the O1s peaks in dependence on the lateral position (plan view) and the emission angle (*z*-axis). The tribostressed area was produced with three tribotracks close to each other with 5 N load, the temperature of the oil bath was 150 °C (data acquired with Theta Probe).

spectra collected within an overnight measurement. The number of steps in the tribological experiment was decreased from 11 to 3 because the XPS-instrument allowed measurements with 30-μm spot size. While the lateral information shows possible lateral inhomogeneities over the tribofilm, the depth information completes the spatial image of the oxygen distribution within the films. The peaks were fitted by constraining the binding energy of the oxide peak to lie between 530.2 and 530.3 eV, the NBO being fixed to be 1.6 eV above the oxide peak, and the BO 3.1 eV above the oxide. The percentages of given oxygen peaks with respect to the sum of all the oxygen peaks are shown in the 3D-plots (figure 9). The colour indicates the three percentages of the oxygen 1s peaks: the lighter the colour, the higher the contribution of this peak to the oxygen signal.

High intensity of the *oxide* was found in the tribostressed region with especially high intensity in the centre of the region, where the contact pressure was higher than at the edge of the contact region. Higher intensity was measured at lower emission angles, implying that the oxide lies mainly at the bottom of the analysed volume. *NBO* was the highest contribution to the oxygen peaks and itself highest at the edge of the tribostressed region. In the tribostressed region its percentage was higher in the outer part of the film while in the non-contact region it was lower in the outer part. The percentage of *BO* was much higher in the thermal film than in the tribofilm. In both cases it was more prominent at higher emission angles, and thus in the outer part of the film.

3.5. Bridging oxygen/non-bridging oxygen

The BO-to-NBO ratio was plotted against both temperature and emission angle (figure 10) to show the film composition, with a focus on the polyphosphates. To determine this ratio, the contribution of oxygen in sulphate groups (four times the corrected intensity of sulphur 2p at 168.8 eV) was subtracted from the NBO peak. At temperatures below 90 °C for tribostressed regions and below 130 °C for non-contact regions the ratio is not plotted, because adsorbed water and hydroxides contributed to the oxygen signal assigned to the BO. At 90 °C and above, a mixture of *ortho*- and pyrophosphates ($P_2O_7^{4-}$, short chain length) is formed in the contact region, the chain length increasing with higher temperature (150 °C: ~2.5 phosphate groups linked together on average) up to a cross-linked polyphosphate at 180 °C (see figure 10, left). In this cross-linked polyphosphate, BO atoms link the chains together; the corresponding phosphorus groups contain then three BO atoms and 1 NBO. The non-contact areas show higher BO/NBO ratios at all temperatures above 130 °C than in the contact regions, meaning that the chains are longer in the non-contacted region. The depth distribution of the polyphosphates can be deduced from the ARXPS measurements (figures 3 and 10, right), where higher ratios are found at higher emission angles for both the non-contact as well as for the tribostressed region. This means that the shorter chains were in the inner part of the film, whereas the longer polyphosphates were to be found near the outside.

3.6. Thickness and composition

In the previous sections it was demonstrated that a multilayered system with depth-dependent composition is present. For this reason the thickness and composition of the adsorbed films have been calculated using a three-layer model [23]. The model is based on the simplifying assumption that the individual layers (oxide layer covered by the reaction layer with an organic layer on top) are homogenous laterally and in depth. The application of this model is discussed in Section 4.

The averaged thicknesses of the reaction and organic layers as a function of the temperature are shown in table 2. The thickness of the non-contact reaction layer increased from 0.9 nm at room temperature up to 5.4 nm at 150 °C. At 180 °C, no iron oxide was detected anymore and therefore the thickness of the overlaying reaction layer must be greater than 6 nm. In the contact region, thicker films than in the non-contact region were formed at temperatures below 110 °C: There was an increase from 1.0 nm at room temperature up to 2.6 nm at 110 °C. Above 110 °C, thinner reaction layers than in

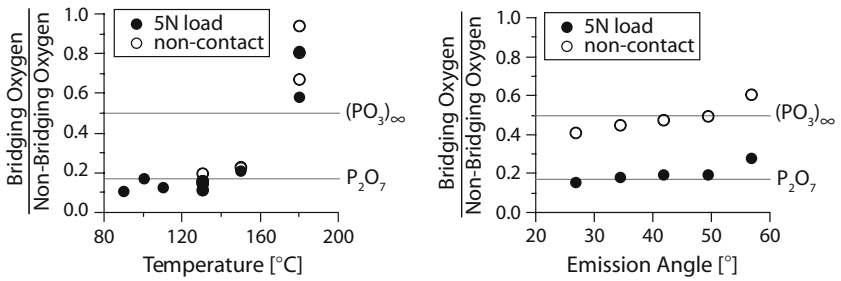

Figure 10. Ratio of bridging oxygen to non-bridging oxygen plotted for areas tribostressed with 5 N load and non-contact regions as a function of temperature (left; PHI 5700) and emission angle (right, temperature: 150 °C; data acquired with Theta Probe).

Table 2.
Layer thicknesses of samples tribostressed in 1 wt.% ZnDTP at different temperatures, calculated for the contact regions produced with 5 N load and the non-contact areas.

T [°C]	Reaction layer (nm)		Organic layer (nm)	
	Non-contact	5 N load	Non-contact	5 N load
25	0.9	1.0	1.9	1.7
60	1.1	1.7	1.2	1.4
90	1.6	2.0	0.4	0.5
100	2.1	2.1	0.6	0.6
110	2.3	2.6	0.4	0.4
130	4.3	2.6	0.7	0.6
150	5.4	2.4	0.7	0.6
180	> 6.0	3.5	2.0	0.8

The reaction layer is on top of the iron oxide and the organic layer is above the reaction layer. Accuracy of the results is estimated to be better than 10%.

the non-contact region were found, the thickness remaining rather constant up to 150 °C and increasing again at 180 °C to a value of 3.5 nm. The thickness of the organic layer after ultrasonic cleaning was between 0.4 and 2.0 nm for both the contact and the non-contact areas.

The ratios of the elements present in the substrate and in the reaction layer were calculated making the assumption of homogenous layers. Below 110°, the substrate in the non-contact regions was a mixture of iron hydroxide and iron oxide with a ratio of O:Fe = 2.6 ± 0.1:1. The same composition was found for the tribostressed region at room temperature. In the contact regions tribostressed at higher temperatures from 60 to 110 °C there was still a mixture of iron hydroxide and iron oxide with a ratio of O:Fe = 1.9 ± 0.1:1, which means that less iron hydroxide but more iron oxide was present. Between 130 and 150 °C a ratio of 1.6 ± 0.3:1 was found for both the non-contact and the tribostressed regions, which is close to a stoichiometry of Fe_2O_3 with O:Fe = 1.5:1. At 180 °C, the ratio in the contact regions was 1.3 ± 0.1:1, which corresponds to Fe_3O_4.

The elemental ratios in the ZnDTP molecule and the reaction layer for both non-contact regions and for samples tribostressed at 5 N load are presented in table 3. In the non-contact area treated at room temperature there was a ratio of P:S of 1:1.9, which is almost that found in pure ZnDTP [38]. The O:P:Fe ratio of 44:1:16 indicates that the oxygen signal is not only coming from adsorbed ZnDTP, but also from the iron hydroxide layer, which has been included into the reaction layer (the iron peaks assigned to iron hydroxide and iron phosphate peaks were taken into account). Going up to 110 °C, the sulphur concentration and zinc:phosphorus ratio increased while iron and oxygen concentrations decreased. The non-contact films at high temperatures (130–150 °C) contained much less oxygen and iron. Furthermore, the content of sulphur is lower than in the ZnDTP molecule, while the zinc concentration is still slightly higher than in ZnDTP. At 180 °C no iron was detected, and sulphur was also present at a very low concentration.

The tribostress led to a depletion of sulphur compared to the original ZnDTP stoichiometry, while the zinc concentration was higher than in ZnDTP, but never as pronounced as in the non-contact areas. At room temperature there was a large amount of iron hydroxide present in the film, but it decreased with higher temperature, while the peak associated with iron phosphate increased slightly.

4. Discussion

4.1. Temperature influence on film thickness and composition

The thickness and the composition of the oxide layer, the reaction layer and the carbon layer were calculated applying a three-layer model [23]. This model was

Table 3.
Elemental ratios of the elements present in the reaction layer normalised by phosphorus.

T [°C]	Non-contact					5 N load				
	O:	P:	S:	Zn:	Fe	O:	P:	S:	Zn:	Fe
ZnDTP	2.0:	1.0:	2.0:	0.5:	0.0					
25	44.0:	1.0:	1.9:	6.1:	15.5	15.2:	1.0:	1.2:	1.6:	3.9
60	29.0:	1.0:	2.6:	7.8:	4.6	7.1:	1.0:	0.6:	1.2:	0.5
90	33.0:	1.0:	6.9:	12.7:	2.7	7.3:	1.0:	0.7:	1.6:	0.6
100	28.0:	1.0:	5.4:	10.4:	1.3	8.9:	1.0:	1.3:	2.5:	0.9
110	15.6:	1.0:	3.5:	6.7:	0.5	6.3:	1.0:	0.8:	1.8:	0.3
130	4.0:	1.0:	1.2:	1.5:	0.1	4.4:	1.0:	0.7:	0.8:	0.3
150	4.5:	1.0:	1.2:	1.9:	0.1	5.7:	1.0:	0.6:	1.2:	0.4
180	3.0:	1.0:	0.1:	0.5:	0.0	4.2:	1.0:	0.4:	0.5:	0.2

In the case of oxygen, the oxide peak and, at temperatures lower than 60 °C, the high-binding-energy peak due to adsorbed water was not taken into account. For iron, only the peaks assigned to iron hydroxide and iron phosphate were attributed to the reaction layer.

applied because ARXPS measurements (oxygen results shown in figures 9 and 10, other elements not shown) suggested the presence of a multilayered system. The roughness could also play a role in the ARXPS profiles but we assumed that no significant influence would be expected between 27 and 54° emission angle on the basis of Gunter's simulations [39]. Higher emission angles are not displayed because these results were affected by elastic scattering [39–41]. In addition, Gunter calculated the ''magic'' emission angle, where surface roughness effects cause minimal effects (accuracy ± 10%), to be equal to 45° [39], which is the emission angle applied in our measurements with the PHI 5700. The authors are aware that the assumption of homogenous layers laterally and in depth is an approximation of the complex reality, but nevertheless the results achieved with this approach can be considered to be more accurate than calculations performed without taking the multilayer structure of the films into account.

The temperature has a significant influence on the film formation for both non-contact (thermal) films and films formed and modified under tribostress (tribofilm). While at low temperatures the reaction layer is very thin (~1–2 nm) for both the thermal and the tribofilm, it becomes thicker upon increasing the temperature, and by 180 °C reaches 2–4 nm in the case of the tribofilm and > 6 nm in the case of the thermal film. The effect of tribological stress depends on the temperature at which the film formation has occurred: Below 100 °C the frictional heat initiates the formation of the reaction layer, the tribological films being thicker than the thermal films. At temperatures > 130 °C, the thermal decomposition of ZnDTP results in thick reaction layers on the surfaces. In these cases, the tribological stress reduces the thickness of the film within the contact region.

The observed reaction layers in the contact region were thinner than films described by other groups [6,8,42], but are in agreement with the short-time experiments with reduced frequency of 5 Hz of Yin *et al.* where they estimated a tribofilm thickness between 2 and 5 nm [19]. The reason for this is most likely the much lower sliding speed of 31 mm/min = 0.0005 m/s applied here, compared to the ~0.1 m/s of Martin *et al.* [20,43]. These values were chosen to place the tribological test squarely within the boundary-lubrication regime: According to Taylor *et al.*, under similar tribological conditions mixed lubrication begins at 0.01 m/s [42]. Another reason could be the different cleaning procedure: while we cleaned the samples ultrasonically in ethanol, Martin *et al.* rinsed them with hexane and propanol and Taylor *et al.* measured *in situ*. Loosely bound phosphate compounds could be washed away from our samples during ultrasonication, while other groups were measuring this layer as well.

The composition of the *iron oxide* below the reaction layer changes with temperature and tribostress. At temperatures below 110 °C, the oxygen-to-iron ratio of 2.6:1 suggests the presence of an iron oxy-hydroxide layer. The composition does not change with tribostress at room temperature, but a reduction of the oxygen content with tribostress could be observed at 60 °C and above. At higher temperatures (130–150 °C), the oxygen from the iron hydroxide layer reacted with the additive, resulting in a substrate covered with an iron oxide layer with a stoichiometry resembling Fe_2O_3. At the very high temperature of 180 °C a further reduction of the oxygen content took place with a resulting composition similar to Fe_3O_4.

The *reaction layer* at *room temperature* in the non-contact regions consists of adsorbed dialkyldithiophosphate molecules on the iron oxy-hydroxide, together with zinc oxide. Both the S:P ratio of 2 (table 3) and the change in the binding energy of sulphur from 162.6 eV in the ZnDTP molecule [38] to 162.1 eV in the surface film support this mechanism. Applying mechanical stress, a reaction layer consisting of zinc orthophosphate $Zn_3(PO_4)_2$, zinc sulphate, zinc oxide, zinc/iron sulphide and thiols is formed. The formation of zinc orthophosphate is indicated by the binding energy of phosphorus, which corresponds to the 133.4 eV found for zinc orthophosphate [36] (see figure 8). It is in agreement with Eglin *et al.* [17].

Increasing the temperature to *60* °C (table 3) also led to surface reactions in the non-contact region: In both non-contact and the contact regions, similar films were found as in the contact region at 25 °C, but with higher amounts of zinc orthophosphate.

At *intermediate temperatures (90–110* °C) thicker reaction layers were formed (see table 2). For both the contact and the non-contact regions they consisted of a mixture of zinc orthophosphate and zinc pyrophosphate $Zn_2P_2O_7$ together with zinc oxide and sulphur. Some of the sulphur was in a higher oxidation state (high binding energy), possibly zinc sulphate, and some was in a low oxidation state (low binding energy), substituting oxygen in the pyrophosphate and/or bound to carbon chains. The presence of iron sulphide and iron disulphide, with the expected binding energy of iron at about 707 eV [44], was not detected. In the contact region there was more zinc phosphate but less zinc sulphate in comparison to the non-contact region. The presence of the *ortho-* and pyrophosphates was determined by the ratio of BO to NBO, which is below 0.166 (see figure 10 left), and the binding energy of phosphorus. The binding energy of phosphorus in the reaction layers was between the reference compounds zinc orthophosphate ($Zn_3(PO_4)_2$: 133.4 eV [36]) and zinc pyrophosphate ($Zn_2P_2O_7$: 133.9 eV [35]) and similar to the binding energy of iron phosphate ($FePO_4$: 133.7 eV [7,35]). This mixture of *ortho-* and pyrophosphates with its average chain length between 1 and 2 is in agreement with Minfray *et al.* [43] and Yin *et al.* [19], who both found a mixture of iron/zinc *ortho-* and pyrophosphates in the bulk

of tribofilms produced at 80 and 100 °C, respectively. Longer chain lengths of 4–10 units were determined by Martin *et al.* at 80 °C using XANES [8].

The reaction layers in the non-contact area at *high temperatures (130–150* °C) consist of a mixture of short-chain zinc polyphosphates, zinc sulphates, thiols and sulphur substituting oxygen in the polyphosphates. The average chain length at 130 °C is 2.5, while at 150 °C it is 3, with increasing chain length towards the outer part of the film (see figures 8 and 10). Longer chains in the outer part of the films were also found by Martin's group at 80 °C [8,43] and by Yin *et al.* at 100 °C [19] using XPS in combination with argon-sputtering and other techniques. The temperature of about 150 °C seems to be quite critical with respect to the resulting chain length, as very long polyphosphate chains were detected in the sample prepared for the angle-resolved measurement. Probably a few degrees difference (accuracy of the oil bath temperature was ± 3 °C) can cause a significant difference in the chain length of the polyphosphate. In the reaction layer of the tribostressed regions, iron with a binding energy of 713.5 eV was found, supporting the presence of iron phosphate. The iron promotes a depolymerisation of the long chains leading to short-chain zinc and iron polyphosphates. Furthermore, a smaller amount of sulphur was found in comparison to the thermal film.

At 180 °C, the thermal films mainly consisted of a cross-linked zinc polyphosphate as indicated both by the BO/NBO ratio, which was higher than 0.5, and the elemental composition. The high-binding-energy peak at 535 eV could then be due to oxygen linking adjacent polyphosphate chains together; similar binding energies of 534.4 ± 0.2 eV were found by Piras *et al.* [38] for samples heated for 126 h in ZnDTP solution at 150 °C. Under tribological stress, small amounts of iron pyrophosphate were formed. This explains the two components found in the phosphorus signal (figure 8), where the high-binding-energy peak (135.3 ± 0.2 eV) corresponds to cross-linked polyphosphate, while the low-binding-energy peak (133.8 ± 0.1 eV) belongs to the iron pyrophosphate. For comparison, linear, non-crosslinked chains of metaphosphate show a binding energy of 135.0 eV [35]. Some minor contributions from sulphates, zinc oxide, thiols and sulphur substituting oxygen in the phosphate were also detected.

4.2. Film-formation mechanism

Based on our measurements on the layer formation described above, we propose the following mechanisms for the different temperatures:

At *room temperature* in the non-contact area, a simple adsorption of the dialkyldithiophosphate took place on the native iron hydroxide surface as Zhang *et al.* suggested as a first step in the mechanism [45]. This was accompanied by zinc oxide, which had been formed during the tribological stress and then deposited in the non-contact area.

At *intermediate and high temperatures* in the non-contact areas, an exchange of the alkyl group from the oxygen to the sulphur atom in the dialkyldithiophosphate molecule occurs at temperatures as low as 60 °C (see figure 11) [13–15]. At higher temperatures in particular, not all alkyl groups bind to the sulphur, but some chains leave the molecule and dissolve in the lubricant solution: While the sulphur in the alkylated thiophosphate remains attached to the molecule, the carbon chain bound to sulphur can leave the phosphate group as a thiol. This is in agreement with Luther *et al.* who found dialkylsulphides, thiols and carbon chains released from ZnDTP during thermal decomposition in the presence of iron [46]. The reaction with a neighbouring phosphoryl group starts to take place at intermediate temperatures [5,16], supported by the presence of pyrophosphate at 90 °C and above. At higher temperatures, this process involves further phosphoryl groups and thus leads to longer polyphosphate chains, until the highly cross-linked polyphosphate is reached at 180 °C. No ion exchange was observed in the non-contact areas. This is in disagreement with Zhang *et al.* [45], who propose the diffusion of iron from the steel into the reaction layer. Free zinc ions react with oxygen from the iron hydroxide at the interface to form zinc oxide or with sulphur to form zinc sulphide (especially at lower temperatures). Furthermore, some of the sulphur becomes oxidised, presumably by O_2 dissolved in the oil, to form the sulphate.

In the tribostressed areas similar reactions occur. The locally higher temperature due to the frictional heat leads to faster thermal reactions compared to those of the non-contact region. In addition, wear and local mixing effects in the tribological contact may lead to the presence of iron oxy-hydroxide particles in the reaction

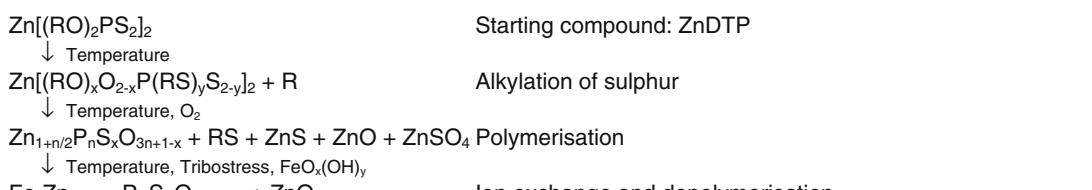

Figure 11. Suggested reaction mechanism of the film formation. *n* designates the phosphate chain length in the non-contact film, which gets depolymerised to a shorter chain length *n*' by the iron in the tribofilm.

film and the oil. This could result in a ligand exchange of the cation in ZnDTP and in the formation of the thermally less stable FeDTP; the iron oxy-hydroxide may catalyse the decomposition of the additive [11,18]. In agreement with this mechanism, under tribological conditions there are tribofilms formed even at room temperature. At temperatures lower than 110 °C, thicker films were observed in the contact regions compared to the non-contact areas, also reflecting the frictional heat contribution to the film formation and the catalytic effect of iron ions. The presence of the high-binding-energy peak in the iron spectrum at 713.5 eV, which is attributed to iron phosphate formation, supports the ligand-exchange mechanism. No indication of the presence of iron sulphide was found. This can be explained on the basis of both the hard and soft acids and bases theory proposed by Martin *et al.* [47] and of thermodynamic considerations presented by Zhang [45], which suggest that even if iron sulphide were to be formed, it would react in the presence of zinc ions or zinc oxide to produce iron ions or iron oxide. Iron has a depolymerisation effect on the polyphosphate chain and forms iron pyrophosphate or iron orthophosphate. This result is substantiated by the fact that at high temperature, shorter-chain-length iron/zinc phosphates are found in the contact region, while longer zinc phosphate chains are formed in the non-contact area.

4.3. Effect of the reaction layer on the friction force

The increasing film thickness at higher temperatures correlates with increasing friction forces in the temperature range from room temperature up to 110 °C (see table 2 and figure 4 right). This might be explained by the fact that during friction at low temperature there are steel–steel contacts as well as contacts including the reaction layer as a friction partner. With increasing temperature, thicker reaction films are formed and therefore fewer steel-steel contacts, with a low friction coefficient, occur, but more contacts with the reaction layer take place, with a high friction coefficient. This results in higher friction coefficients with thicker reaction layers. After reaching a reaction-layer thickness of 2.6 nm at 110 °C, both the layer thickness and the friction force are found to be constant with increasing temperature. This might be interpreted as a result of the coating of both sliding partners with a reaction layer at these temperatures. In addition, the composition of the layer changes from short-chain phosphates at lower temperatures to longer chains at higher temperatures—this may also influence the friction force via the likely higher viscosity of the reaction layer.

The high-temperature friction coefficient, 0.2, is high in comparison with values of lower than 0.1 measured under boundary lubrication conditions for fully formulated lubricants [20]. To reduce the friction force, friction modifiers such as molybdenum dialkyldithiocarbamate (MoDTC) are added to the lubricant in high-performance motor oils [20,48].

5. Conclusion

The thickness and the composition of non-contact and tribostressed films in the steel/ZnDTP system could be analysed in a non-destructive way, both laterally and as a function of the layer depth, by means of small-area, imaging and ARXPS.

Strong temperature dependences of both the oxide and the reaction layer were observed: the oxide layer at low temperatures was found to be an iron oxy-hydroxide. At higher temperature the stoichiometry of the substrate was very close to the Fe_2O_3 and at 180 °C similar to Fe_3O_4.

The thickness of the reaction layer increased with increasing temperature, reaching values greater than 6 nm in the non-contact region and 4 nm in the contact area. Its composition changed from adsorbed dialkyldithiophosphate at room temperature through a short-chain zinc phosphate at intermediate temperature to a cross-linked polyphosphate at 180 °C. Under tribological stress the tribofilm was formed even at room temperature, where it consisted of zinc orthophosphate. Increasing temperature led to longer chains. These were shortened in the contact regions due to reaction with the iron ions, which could be incorporated into the tribofilm. This leads to a mixture of iron and zinc phosphates. Longer chains were found in the outer part of the reaction layers by means of ARXPS.

The friction force correlates with the thickness and composition of the anti-wear film: the thicker the film, the longer the phosphate chains and the higher the friction coefficient.

References

[1] D. Dowson, C.M. Taylor and G. Zhu, J. Phys. D: Appl. Phys. 25 (1992) A313.
[2] S. Einecke, C. Schulz and V. Sick, Appl. Phys. B 71 (2000) 717.
[3] A. Hugnell and S. Andersson, Wear 179 (1994) 101.
[4] A. Hugnell, S. Bjorklund and S. Andersson, Wear 199 (1996) 202.
[5] H. Spikes, Tribol. Lett. 17 (2004) 469.
[6] S. Bec, A. Tonck, J.M. Georges, R.C. Coy, J.C. Bell and G.W. Roper, Proc. R. Soc. London, A 455 (1999) 4181.
[7] M. Eglin, A. Rossi and N.D. Spencer, Tribol. Lett. 15 (2003) 199.
[8] J.M. Martin, C. Grossiord, T. Le Mogne, S. Bec and A. Tonck, Tribol. Int. 34 (2001) 523.
[9] Z.F. Yin, M. Kasrai, G.M. Bancroft, K.F. Laycock and K.H. Tan, Tribol. Int. 26 (1993) 383.
[10] M.L.S. Fuller, L.R. Fernandez, G.R. Massoumi, W.N. Lennard, M. Kasrai and G.M. Bancroft, Tribol. Lett. 8 (2000) 187.
[11] F.M. Piras, A. Rossi and N.D. Spencer, *Proceedings of 28th Leeds-Lyon Symposium, Vienna, 2001* (Elsevier Science B.V., Amsterdam, 2002) 199.
[12] F.M. Piras, A. Rossi and N.D. Spencer, Langmuir 18 (2002) 6606.
[13] R.C. Coy and R.B. Jones, ASLE Trans. 24 (1981) 77.

[14] R.B. Jones and R.C. Coy, ASLE Trans. 24 (1981) 91.
[15] M.L.S. Fuller, M. Kasrai, G.M. Bancroft, K. Fyfe and K.H. Tan, Tribol. Int. 31 (1998) 627.
[16] M.A. Nicholls, T. Do, P.R. Norton, M. Kasrai and G.M. Bancroft, Tribol. Int. 38 (2005) 15.
[17] M. Eglin, A. Rossi and N.D. Spencer, *Proceedings of 28th Leeds-Lyon Symposium, Vienna, 2001* (Elsevier Science B.V., Amsterdam, 2002) 49.
[18] H. Fujita and H.A. Spikes, Proc. Inst. Mech. Eng. J 218 (2004) 265.
[19] Z.F. Yin, M. Kasrai, M. Fuller, G.M. Bancroft, K. Fyfe and K.H. Tan, Wear 202 (1997) 172.
[20] M.I. De Barros, J. Bouchet, I. Raoult, T. Le Mogne, J.M. Martin, M. Kasrai and Y. Yamada, Wear 254 (2003) 863.
[21] R.K. Brow, J. Non-Cryst. Solids 263 (2000) 1.
[22] M. Eglin, A. Rossi and N.D. Spencer, Tribol. Lett. 15 (2003) 193.
[23] A. Rossi and B. Elsener, Surf. Interface Anal. 18 (1992) 499.
[24] J.H. Scofield, J. Electron Spectrosc. 8 (1976) 129.
[25] K. Berresheim, M. Matternklosson and M. Wilmers, Fresenius. J. Anal. Chem. 341 (1991) 121.
[26] S. Tanuma, C.J. Powell and D.R. Penn, Surf. Interface Anal. 21 (1993) 165.
[27] S. Tanuma, C.J. Powell and D.R. Penn, Surf. Interface Anal. 35 (2003) 268.
[28] K. Laajalehto, I. Kario and P. Nowak, Appl. Surf. Sci. 81 (1994) 11.
[29] H. Konno, K. Sasaki, M. Tsunekawa, T. Takamori and R. Furuichi, Bunseki Kagaku 40 (1991) 609.
[30] D. Zerulla and T. Chasse, Langmuir 15 (1999) 5285.
[31] K. Heister, M. Zharnikov, M. Grunze, L.S.O. Johansson and A. Ulman, Langmuir 17 (2001) 8.
[32] K. Matsumoto, *Surface chemical and tribological investigations of phosphorus-containing lubricant additives*, Ph.D. Thesis (ETH Zurich, Zurich, Switzerland, 2003).
[33] C.R. Brundle, T.J. Chuang and K. Wandelt, Surf. Sci. 68 (1977) 459.
[34] M. Olla, G. Navarra, B. Elsener and A. Rossi, Surf. Interface Anal. 38 (2006) 964.
[35] R. Pinna, *Synthesis and characterization of Zn and Fe polyphosphates glasses*, Diploma Thesis (University of Cagliari, Cagliari, Italy, 2001/2002).
[36] E.C. Onyiriuka, J. Non-Cryst. Solids 163 (1993) 268.
[37] R.K. Brow, C.M. Arens, X. Yu and E. Day, Phys. Chem. Glasses 35 (1994) 132.
[38] F.M. Piras, A. Rossi and N.D. Spencer, Tribol. Lett. 15 (2003) 181.
[39] P.L.J. Gunter, O.L.J. Gijzeman and J.W. Niemantsverdriet, Appl. Surf. Sci. 115 (1997) 342.
[40] C.J. Powell, A. Jablonski, S. Tanuma and D.R. Penn, J. Electron Spectrosc. 68 (1994) 605.
[41] M.P. Seah and I.S. Gilmore, Surf. Interface Anal. 31 (2001) 835.
[42] L. Taylor, R. Glovenea, M. Ribeaud and H.A. Spikes, *Proceedings of International Tribology Conference, Nagasaki* (Japanese Society of Tribologists, 2000) 1257.
[43] C. Minfray, J.M. Martin, C. Esnouf, T. Le Mogne, R. Kersting and B. Hagenhoff, Thin Solid Films 447 (2004) 272.
[44] P. de Donato, C. Mustin, R. Benoit and R. Erre, Appl. Surf. Sci. 68 (1993) 81.
[45] Z. Zhang, E.S. Yamaguchi, M. Kasrai, G.M. Bancroft, X. Liu and M.E. Fleet, Tribol. Lett. 19 (2005) 221.
[46] H. Luther, S.K. Sinha, Erdgas Erdoel Kohle, Petrochemistry 17 (1964) 91.
[47] J.M. Martin, Tribol. Lett. 6 (1999) 1.
[48] S. Bec, A. Tonck, J.M. Georges and G.W. Roper, Tribol. Lett. 17 (2004) 797.
[49] E. 673-03, *Standard Terminology Relating to Surface Analysis* (ASTM International, West Conshohocken, US, 2003).
[50] D. Briggs and J.T. Grant, *Surface Analysis by Auger and X-Ray Photoelectron Spectroscopy* (IM Publications and Surface Spectra Limited, Chichester/Manchester UK, 2003).
[51] D.R. Lide, *The CRC Handbook of Chemistry and Physics* (CRC Press, Boca Raton, 2004).
[52] M. Altaf, M. Ashraf Chaudhry, M. Shakeel Bilal and M. Ashfaq Ahmad, J. Res. Sci. 13 (2002) 9.
[53] G. Navarra, A. Falqui, G. Piccaluga and G. Pinna, Phys. Chem. Chem. Phys. 4 (2002) 4817.
[54] E.A. Cho, H. Kwon and D.D. Macdonald, Electrochim. Acta 47 (2002) 1661.